

## Electronic properties of $(\text{ZnSe})_m(\text{Cd}_{1-x}\text{Zn}_x\text{Se})_n$ superlattices

Shang-Fen Ren, Zhong-Quan Gu,\* and Yia-Chung Chang

Department of Physics and Materials Research Laboratory, University of Illinois at Urbana-Champaign, Urbana, Illinois 61801

(Received 28 May 1993; revised manuscript received 4 October 1993)

We present theoretical calculations on the electronic structures of  $(\text{ZnSe})_m(\text{Cd}_{1-x}\text{Zn}_x\text{Se})_n$  superlattices. First-principle pseudopotential calculations are performed to obtain the valence-band offset for CdSe grown on ZnSe. We then use an empirical nonlocal pseudopotential method, including the spin-orbit interaction to calculate the band structures and effective masses of  $(\text{ZnSe})_m(\text{Cd}_{1-x}\text{Zn}_x\text{Se})_n$  superlattices grown on ZnSe. The empirical pseudopotentials are taken to be linear combinations of Gaussian functions with a few adjustable parameters. The parameters of ZnSe and CdSe are fitted to available experimental data. The effects of strain due to lattice mismatch have been properly taken into account. We have also studied the band gap as a function of composition and layer thicknesses of constituent materials in superlattices. The results are in agreement with recent experimental data.

Recently, in searching for a material that is more efficient for light emission in the blue-green range, extensive studies of II-VI semiconductors, their alloys, and their alloy superlattices have been performed.<sup>1-3</sup> Among these materials,  $(\text{ZnSe})_m(\text{Cd}_{1-x}\text{Zn}_x\text{Se})_n$  superlattices have attracted much attention. In this paper, we report theoretical studies on the electronic properties of zinc-blende CdSe and  $(\text{ZnSe})_m(\text{Cd}_{1-x}\text{Zn}_x\text{Se})_n$  superlattices using both first-principles and empirical pseudopotential methods.

In order to obtain the correct band structure and optical properties for ZnSe-CdSe superlattice systems, information about the band offset at the interface is needed. We have carried out a first-principles self-consistent pseudopotential calculation for the band offset for the (001) ZnSe-CdSe interface, which is based on the approach developed by Pickett, Louie, and Cohen,<sup>4</sup> Kunc and Martin,<sup>5</sup> and Van de Walle and Martin.<sup>6</sup> In this approach, self-consistent charge densities are properly calculated. The charge transfer across the interface leads to an interface dipole which is responsible for the band discontinuity.

Our calculations are performed for a supercell geometry, which consists of three layers of cubic ZnSe and three layers of strained CdSe, including a total of 12 atoms. The CdSe layers are compressed parallel to the interface to match the ZnSe lattice constant (5.668 Å), and expanded in the perpendicular direction to reduce the elastic energy. Following Van der Walle and Martin,<sup>6</sup> we determine the lattice constants by a macroscopic elastic theory. For strained CdSe layers, the lattice constant in the growth direction is 6.521 Å.

The norm-conserving, *ab initio* pseudopotentials for Zn, Cd, and Se were generated in configurations listed in Table I. Both the Zn 3*d* electrons and the Cd 4*d* electrons were treated as core electrons in these configurations, but the core exchange-correlation corrections were taken into account according to procedures described in Ref. 7. Although these electrons are corelike in the elemental metals, they may fall within the valence-band region in compounds and play a role in bonding.

Wei and Zunger<sup>8</sup> have found that these semicore *d* states have an important effect on the valence-band offset (VBO) of the III-V and II-VI semiconductors. Recently, Qteish and Needs<sup>9</sup> argued that accurate results can be obtained with the shallow cation *d* states treated as core states, provided the core exchange-correlation corrections are included. Since the relaxation for Zn 3*d* and Cd 4*d* states can cause some convergence problems for the band structure at *k* points near the zone center, we adopted the scheme of Qteish and Needs<sup>9</sup> to estimate VBO in the ZnSe-CdSe superlattice. To make sure the configurations chosen are correct for our present system, we have made a test calculation for bulk ZnSe with kinetic energy up to 18 Ry. The calculated valence-band eigenvalues at high symmetry points in the Brillouin zone are given in Table II, together with the results calculated by Bernard and Zunger<sup>10</sup> (in parentheses) using an all-electron mixed-basis approach for comparison. The agreement between the two calculations is satisfactory.

To estimate the potential shift at the interface accurately, more than 900 plane waves with energy cutoff at 9 Ry were included in the expansion of the wave functions. Four special points were used for sampling in *k* space. Convergence for the self-consistent potential was achieved with a difference of less than  $10^{-5}$  Ry between the last two iterations. The potential shift at the interface is 0.8952 eV, forming an upward step from ZnSe to CdSe.

To line up the band structure on both sides of the interface, we have to perform the band calculation for bulk materials with the same crystal structures as in the superlattice layers. They are zinc-blende ZnSe and strained CdSe. The positions of the topmost valence bands with

TABLE I. Configuration for generating norm-conserving pseudopotentials.

	Zn	Cd	Se
<i>s</i>	$4s^2$	$5s^2$	$4s^2 4p^4$
<i>p</i>	$4s^{0.75} 4p^{0.25}$	$5s^{0.75} 5p^{0.25}$	$4s^2 4p^4$
<i>d</i>	$4s^{0.75} 4d^{0.25}$	$5s^{0.75} 5d^{0.25}$	$4s^1 4p^{2.75} 4d^{0.25}$

TABLE II. Calculated valence-band eigenvalues at high-symmetry points for ZnSe (in eV). The corresponding values obtained by Bernard and Zunger (Ref. 10) are included in parentheses.

$\Gamma_{1v}$	-12.96(-12.86)	$X_{1v}$	-11.55(-11.79)	$L_{1v}$	-11.91(-12.06)
$\Gamma_{15v}$	0.00(0.00)	$X_{3v}$	-4.73(-4.82)	$L_{1v}$	-4.92(-5.21)
		$X_{5v}$	-1.90(-2.20)	$L_{3v}$	-0.73(-0.87)

respect to their average potentials are 6.9975 and 6.4331 eV, respectively, for ZnSe and strained CdSe. Combining these results, we determined the valence-band offset to be 0.331 eV without including spin-orbit interaction.

The spin-orbit interaction was added to the Hamiltonian as a perturbation and the spin-orbit splitting was calculated in first-order approximation. With the spin-orbit interaction the sixfold-degenerate valence band of cubic ZnSe at  $\Gamma$  split into a high-lying fourfold multiplet (up 0.1416 eV) and a lower-lying twofold multiplet (down 0.2833 eV). For strained CdSe, the spin-orbit interaction shifts the topmost valence band upward by 0.1390 eV, almost the same value as in ZnSe. Therefore the net effect of the spin-orbit coupling on band offset is negligible in this particular situation.

We have noticed slow VBO convergence with respect to the thickness of the slab of each material.<sup>9</sup> Since the main purpose of this paper is to extract an overall picture of the  $(\text{ZnSe})_m(\text{Cd}_{1-x}\text{Zn}_x\text{Se})_n$  superlattices, only a reasonably accurate VBO is required. Therefore, as mentioned before, only  $3 \times 3$  superlattice geometry was employed to calculate the VBO. Test calculations indicate that the band structures are not sensitive to changes of VBO within 0.2 eV.

By using the above result for the ZnSe/CdSe band offset from first-principles calculation, we have performed systematic studies of  $(\text{ZnSe})_m(\text{Cd}_{1-x}\text{Zn}_x\text{Se})_n$  superlattices with an empirical pseudopotential method. In this method, both local and nonlocal pseudopotentials are taken to be linear combinations of Gaussian functions with a few adjustable parameters. Our local potentials take the form  $V_L = v_1 e^{-\alpha_1 r^2} + v_2 r^2 e^{-\alpha_2 r^2} + v_3 e^{-\alpha_3 r^2}$ , where  $v_1, v_2, v_3$  are adjustable parameters, while  $\alpha_1$  and  $\alpha_3$  are fixed at 0.5588 and 0.2747 a.u. for anions and 0.4381 and 0.2154 a.u. for cations. The nonlocal potentials take the form  $V_{NL} = \sum_{lm} A_l e^{-(r/R_c)^2} |lm\rangle\langle lm|$ , where  $A_l$  for different angular momentum  $l$  are adjustable parameters and the core radius  $R_c$  is fixed at 2.3 a.u. The spin-orbit coupling in each material is also included empirically in the form

$$V_{\text{SO}} = \lambda \sum_{b,b'} |b\rangle\langle b|\sigma \cdot \mathbf{L}|b'\rangle\langle b'|,$$

where  $\langle r|b\rangle = \{x, y, z\} e^{-(r/R_c)^2} / \sqrt{S}$  denote three effective  $p$ -like core orbitals,  $S$  being the normalization constant. The parameters for both CdSe and ZnSe are first obtained by fitting the screened atomic pseudopotential of Cd, Zn, and Se calculated by first principles, and then adjusting them to fit the available experimental data for the band structure. For zinc-blende CdSe, the pseudopotentials are fitted to the measured band gaps at  $\Gamma$ ,  $L$ , and  $X$  and the dielectric functions,<sup>11</sup> and for ZnSe they are fitted to experimental data reported in Ref. 12. The results are shown in Table III.

The band structure of unstrained zinc-blende CdSe has been reported in Ref. 11. The band structure of strained zinc-blende CdSe grown on ZnSe buffer layers is shown in Fig. 1, in which the lattice constant in the in-plane direction is 5.668 Å and in the growth direction is 6.521 Å. Because of biaxial strain, the band structure in the [100] direction is different from that in the [001] direction, so the band structures in both directions are shown. Table IV shows the valence-to-conduction transition energies at high symmetry points and the zone-center spin-orbit splitting ( $\Delta_0$ ) for unstrained CdSe, strained CdSe (on ZnSe), and ZnSe, all calculated by the empirical pseudopotential method.  $E_0$ ,  $E_1$ , and  $E_2$  denote the band gaps at  $\Gamma$ ,  $L$ , and  $X$ , respectively.

Because of the mismatch of the lattice constants between CdSe and ZnSe, the superlattices of interest grown on thick ZnSe buffer layers will always be strained, as we described above. The alloy part of the superlattices is approximated by a virtual crystal of which the parameters are averaged according to the composition. The bulk band structures for ZnSe and strained zinc-blende CdSe obtained by using the parameters listed in Table III have an automatic band offset of 0.71 eV, and the band offset obtained by the first-principles calculation is 0.33 eV. To include the effect due to the correction in band offset, we add to the superlattice potential a Kronig-Penney potential of the form

TABLE III. Parameters of ZnSe and CdSe in the nonlocal pseudopotential methods (in a.u.).

	$v_{1c}$	$v_{2c}$	$v_{3c}$	$v_{1a}$	$v_{2a}$	$v_{3a}$		
ZnSe	1.14	-0.72	-0.74	2.55	-1.60	-1.65		
CdSe	1.35	-0.85	-0.87	2.55	-1.60	-1.65		
	$A_{0c}$	$A_{1c}$	$A_{2c}$	$A_{0a}$	$A_{1a}$	$A_{2a}$	$\lambda_a$	$\lambda_c$
ZnSe	-0.15	-0.02	0.57	-0.105	0.2	0	0.000385	0.000059
CdSe	0	-0.12	1.3	0	0.3	0	0.000256	0.000121

TABLE IV. Transition energies and spin-orbit splitting in zinc-blende CdSe and ZnSe bulk material (in eV).

	$E_0$	$E_1$	$E_2$	$\Delta_0$	$\Delta_1$	$\Delta_2$
ZnSe	2.714	4.582	6.187	0.43	0.30	0.28
CdSe	1.660	4.217	6.058	0.39	0.28	0.19

$$V_{\text{KP}}(z) = \begin{cases} -V_0(1-x), & z \text{ in } \text{Cd}_{1-x}\text{Zn}_x\text{Se} \text{ region,} \\ 0, & z \text{ in ZnSe region,} \end{cases}$$

where  $V_0$  is the correction in band offset. In the present case, this correction is 0.38 eV.

The  $(\text{ZnSe})_3(\text{CdSe})_1$  superlattice has recently been demonstrated to play an important role in making blue-green quantum-well lasers.<sup>13</sup> The  $(\text{ZnSe})_3(\text{CdSe})_1$  superlattice can also be viewed as a new bulk material (a “digital alloy”) which is then used with ZnSe to make quantum-well structures. For the purpose of understanding these structures, we need to know the band structures and effective masses of the constituent materials, namely,  $(\text{ZnSe})_3(\text{CdSe})_1$  and ZnSe. Since interdiffusion is usually unavoidable during material growth, we consider several  $(\text{ZnSe})_m(\text{Cd}_{1-x}\text{Zn}_x\text{Se})_n$  superlattices with the overall CdSe composition equal to 25%, which model the  $(\text{ZnSe})_3(\text{CdSe})_1$  superlattice with varying degree of interdiffusion. The band structure of  $(\text{ZnSe})_3(\text{CdSe})_1$  for wave vectors along the [100] and [001] directions is shown in Fig. 2. The effective masses at  $\Gamma$  along the [001], [100], and [110] directions for the above two superlattices plus the  $(\text{ZnSe})_1(\text{Cd}_{0.33}\text{Zn}_{0.67}\text{Se})_3$  superlattice and the  $(\text{Cd}_{0.25}\text{Zn}_{0.75}\text{Se})$  alloy are shown in Table V. Due to spin splitting along low-symmetry axes, the valence-band structure near  $\Gamma$  is approximated by the expression  $E_i(k) - E_k(0) = \hbar^2 k^2 / 2m^* + \alpha_i k$ ; where  $i = \text{hh, lh, and sp}$  for heavy-hole, light-hole, and split-off bands respectively. The effective masses ( $m^*$ ) along these directions are calculated by using the energy averaged over the two spin-split bands, and all the effective masses and the split-

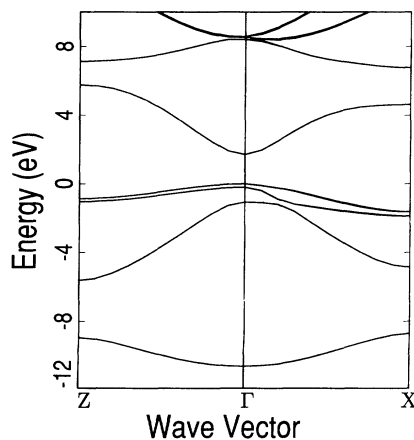


FIG. 1. Band structure of zinc-blende CdSe grown on a thick ZnSe buffer layer (strained), where  $x$  is the in-plane direction, and  $z$  is the growth direction.

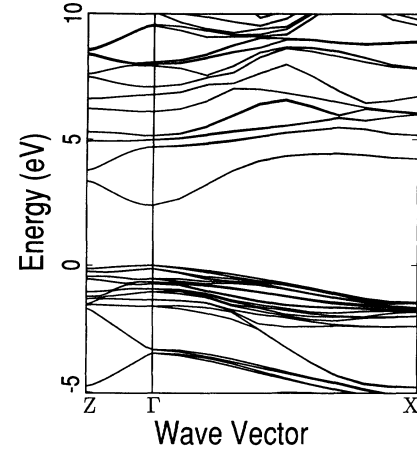


FIG. 2. Band structure of the  $(\text{ZnSe})_3(\text{CdSe})_1$  superlattice.

ting constants ( $\alpha_i$ ) are evaluated at 3% of the bulk Brillouin zone.  $\Delta_{\text{hl}}$  in this table denotes the energy differences between the heavy- and light-hole bands at  $\Gamma$ .

So far all our calculations have been performed for room temperature. Finally, we study the trend of band gaps for superlattices with different numbers of CdSe or ZnSe layers at zero temperature. At zero temperature the band gap is increased; thus, we increased the nonlocal parameter ( $A_0$ ) by 0.03 a.u. so that the band gaps of CdSe and ZnSe become 1.753 and 2.821 eV, respectively, in agreement with experiment. Figure 3 shows the fundamental band gaps of  $(\text{ZnSe})_m(\text{CdSe})_n$  superlattices as a function of  $m$  (number of ZnSe layers) for different values of  $n$ . The arrows indicate the limiting values of the band gap in the quantum-well limit (i.e.,  $n \rightarrow \infty$ ), which are obtained by extrapolation of the function  $E_g(m) = E_g(\infty)(1 - ae^{-am})$ . The band gap of CdSe/ZnSe quantum wells as a function of the number of CdSe layers is in agreement with recent experimental findings.<sup>14</sup>

In summary, we have performed theoretical studies of the electronic band structures of  $(\text{ZnSe})_m(\text{Cd}_{1-x}\text{Zn}_x\text{Se})_n$

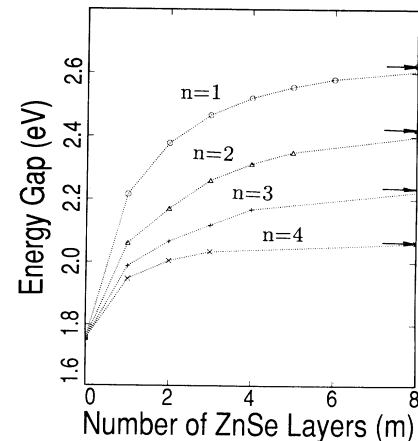


FIG. 3. Band gap of  $(\text{ZnSe})_m(\text{CdSe})_n$  superlattices grown on a ZnSe buffer layer as a function of the number of ZnSe layers in the superlattice.

TABLE V. Energy gap and splitting at the  $\Gamma$  point (in eV), and effective masses (in  $m_e$ ), in four  $(\text{ZnSe})_m(\text{Cd}_x\text{Zn}_{1-x}\text{Se})_n$  superlattices with overall 25% CdSe.

	Energy	Direction	$m_{\text{sp}}$	$m_{\text{lh}}$	$m_{\text{hh}}$	$m_e$	$\alpha_{\text{sp}}$	$\alpha_{\text{lh}}$	$\alpha_{\text{hh}}$
$(\text{ZnSe})_3(\text{CdSe})_1$	$E_g = 2.368$	[01]	0.41	0.41	1.28	0.16	0	0	0
$a_{\parallel} = 5.668 \text{ \AA}$	$\Delta_0 = 0.526$	[100]	1.07	0.37	0.29	0.16	0.50	0.17	0.03
$a_{\perp} = 5.881 \text{ \AA}$	$\Delta_{\text{hl}} = 0.135$	[110]	1.17	0.44	0.27	0.17	0.56	0.24	0.01
$(\text{ZnSe})_2(\text{Cd}_{0.5}\text{Zn}_{0.5}\text{Se})_2$	$E_g = 2.467$	[001]	0.27	0.36	1.24	0.16	0	0	0
$a_{\parallel} = 5.668 \text{ \AA}$	$\Delta_0 = 0.526$	[100]	0.70	0.39	0.29	0.16	0.20	0.12	0.01
$a_{\perp} = 5.880 \text{ \AA}$	$\Delta_{\text{hl}} = 0.125$	[110]	0.67	0.34	0.34	0.17	0.17	0.11	0.01
$(\text{ZnSe})_1(\text{Cd}_{0.33}\text{Zn}_{0.67}\text{Se})_3$	$E_g = 2.506$	[001]	0.26	0.35	1.23	0.16	0	0	0
$a_{\parallel} = 5.668 \text{ \AA}$	$\Delta_0 = 0.522$	[100]	0.60	0.39	0.29	0.17	0.10	0.08	0.01
$a_{\perp} = 5.879 \text{ \AA}$	$\Delta_{\text{hl}} = 0.121$	[110]	0.58	0.34	0.34	0.17	0.07	0.07	0.01
$(\text{Cd}_{0.25}\text{Zn}_{0.75}\text{Se})_4$	$E_g = 2.520$	[001]	0.23	0.34	1.33	0.16	0	0	0
$a_{\parallel} = 5.668 \text{ \AA}$	$\Delta_0 = 0.519$	[100]	0.47	0.39	0.30	0.17	0.07	0.07	0.01
$a_{\perp} = 5.879 \text{ \AA}$	$\Delta_{\text{hl}} = 0.093$	[110]	0.51	0.35	0.34	0.17	0.06	0.06	0.01

superlattices by using both first-principles and empirical pseudopotential methods. The valence-band offset between ZnSe and CdSe is found to be 0.33 eV. Effective masses and spin splitting along various symmetry directions for the  $(\text{ZnSe})_3(\text{CdSe})_{12}$  superlattice are predicted, and the effects due to interdiffusion are examined. This information is important for modeling the performance of quantum-well laser structures made of  $(\text{ZnSe})_3(\text{CdSe})_1$  and ZnSe. We have also examined the fundamental band

gaps of  $(\text{ZnSe})_m(\text{CdSe})_n$  superlattices as functions of  $m$  and  $n$ , and our results are in agreement with recent experimental findings.

We would like to thank Dr. Hong Luo and Dr. J. J. Song for many fruitful discussions. This work was supported by the U.S. Office of Naval Research (ONR) under Contract No. N00014-90-J-1267.

\*Permanent address: Institute of Semiconductors, Chinese Academy of Sciences, Beijing 100083, China.

<sup>1</sup>H. Jeon, J. Ding, A. V. Nurmikko, H. Luo, N. Samarth, J. K. Furdyna, W. A. Bonner, and R. E. Nahory, *Appl. Phys. Lett.* **57**, 2413 (1990).

<sup>2</sup>M. A. Haase, J. Qiu, J. M. DePuydt, and H. Cheng, *Appl. Phys. Lett.* **59**, 1272 (1991).

<sup>3</sup>Z. Hu, J. Ren, B. Sneed, K. A. Bowers, K. J. Gossett, C. Boney, Y. Lansari, J. W. Cook, Jr., J. F. Schetzina, G. C. Hua, and N. Otsuka, *Appl. Phys. Lett.* **16**, 1266 (1992).

<sup>4</sup>W. E. Pickett, S. G. Louie, and M. L. Cohen, *Phys. Rev. B* **17**, 815 (1978).

<sup>5</sup>K. Kunc and R. M. Martin, *Phys. Rev. B* **24**, 3445 (1981).

<sup>6</sup>C. G. Van de Walle and R. M. Martin, *Phys. Rev. B* **34**, 5621 (1986).

<sup>7</sup>S. G. Louie, S. Froyen, and M. L. Cohen, *Phys. Rev. B* **26**, 1738 (1982).

<sup>8</sup>S. H. Wei and A. Zunger, *Phys. Rev. Lett.* **59**, 144 (1987).

<sup>9</sup>A. Qteish and R. J. Needs, *Phys. Rev. B* **43**, 4229 (1991).

<sup>10</sup>J. E. Bernard and A. Zunger, *Phys. Rev. B* **36**, 3199 (1987).

<sup>11</sup>Y. D. Kim, M. L. Klein, S. F. Ren, Y. C. Chang, H. Luo, N. Samarth, and J. K. Furdyna, *Phys. Rev. B* (to be published).

<sup>12</sup>*Physics of II-VI and I-VII Compounds, Semimagnetic Semiconductors*, edited by a Modelung, Landolt-Börnstein, New Series, Group III, Vol. 17, Part B (Springer-Verlag, Berlin, 1982).

<sup>13</sup>H. Luo, N. Samarth, A. Yin, A. Pareek, M. Dobrowolska, J. K. Furdyna, K. Mahalingam, N. Otsuka, F. C. Peiris, and J. R. Buschert, *J. Electron. Mater.* **22**, 467 (1993).

<sup>14</sup>J. J. Song (private communication).